

Postsynthesis Modification of Aluminophosphates by Reaction with Silicon Tetrachloride

JEFFREY L. BRINEN¹ AND MARK G. WHITE²

School of Chemical Engineering, Georgia Institute of Technology, Atlanta, Georgia 30332-0100

Received July 28, 1989; revised January 30, 1990

Silicon tetrachloride was reacted with fixed beds of AlPO₄-5 at temperatures between 450 and 750°C. Crystalline samples which showed properties different from the parent AlPO₄-5 materials resulted from most treatments. Samples were prepared with silicon mole fractions between 0.04 to 0.11 and oxygen monolayer volumes between 19.6 and 82.2 STP cm³/g. The samples showed increasing silicon content and decreasing oxygen monolayer volumes for increasing treatment temperature. The samples showing the smaller O₂ monolayer volumes may have silicon-rich material in the pores.

Crystalline, aluminum phosphate (AlPO₄-5), and the modified samples were characterized by ammonia titration, pyridine IR spectroscopy, and two probe reactions: toluene methylation and cumene cracking. These SiCl₄-treated samples showed ammonia retentions 50-80% greater than those of the untreated sample and toluene methylation activities three to four times that of the untreated AlPO₄-5. However, the SiCl₄ treatment conferred to the samples no increase in cumene cracking rates and the pyridine IR spectra over the modified samples showed only Lewis-bound pyridine, which was observed in the untreated AlPO₄-5. The xylene product distribution for the methylation reaction over the modified AlPO₄-5 (*o/p/m* = 0.51/0.27/0.22) was similar to that expected for a Friedel-Crafts alkylation (*o/p/m* = 0.54/0.29/0.17). © 1990 Academic Press, Inc.

INTRODUCTION

Researchers at Union Carbide described a family of crystalline, microporous materials having equimolar amounts of Al₂O₃ and P₂O₅ (1, 2). The family of aluminophosphates is designated by AlPO₄-*n*, where *n* distinguishes between the structures. The crystal structures of a few of these materials are known and the one designated as AlPO₄-5 shows hexagonal symmetry (cell constants: *a* = 1.373 nm, *c* = 0.848 nm, {*γ*} = 120°; unit cell composition, 12 AlPO₄-*n* · H₂O). This structure contains channels parallel to the *c*-axis (3) which are formed by 12-membered rings of alternating AlO₄ and PO₄ tetrahedra. The framework is neutral; however, the structure is considered polar due to strict alternation of the alumina and

phosphate tetrahedra. As such the AlPO₄-5 material is hydrophobic compared to the other zeolites and molecular sieves showing anionic frameworks. Moreover, the material shows very low reactivity to cumene cracking (4) and butane cracking (5).

Subsequently, Union Carbide announced a related family of crystalline, microporous materials known as silicoaluminophosphates which were designated as SAPO-*n* (6). This new family contains some structures common to the AlPO₄-*n* family for *n* = 5, 11, 16, and 31 plus other structures common to erionite (SAPO-17) and sodalite (SAPO-20) (5). The SAPO materials have tetrahedral oxide frameworks of silicon, aluminum, and phosphorus. The structure of SAPO-37 has been studied by Saldarriaga *et al.* (7) using NMR and FTIR. They showed that silicon substitutes for phosphorus in the hypothetical aluminophosphate framework of the faujasite structure and that there is a regular distribution of silicon, aluminum, and phosphorus in the

¹ Present address: Research Engineer, Exxon Chemical Co., 5200 Bayway Drive, Baytown, TX 77522-5200.

² To whom correspondence should be addressed.

negatively charged structure. The SAPO-37 calcined in air shows acidic sites. Indeed, Lok *et al.* (5) reported butane cracking activities for SAPO-37 which were 20 times that of $\text{AlPO}_4\text{-5}$.

One member of the $\text{AlPO}_4\text{-}n$ family has been modified to change its adsorption properties. $\text{AlPO}_4\text{-5}$ has been reacted with silicon tetrachloride at temperatures near 600°C (8). This same treatment has been used to dealuminate molecular sieves (9). The silicon tetrachloride treatment incorporated small amounts of silicon (ca. 0.6 wt%) into the materials such that the N_2 and water adsorptions were smaller than that of the parent $\text{AlPO}_4\text{-5}$. Although the treatment decreased the ammonia pickup relative to the $\text{AlPO}_4\text{-5}$, the treated solid showed stronger sorption of the base. This technique appeared to have merit for altering the properties of the parent $\text{AlPO}_4\text{-}n$. Thus, we explored the silicon tetrachloride technique in detail.

We present here a study of the reaction between a gaseous mixture of silicon tetrachloride in nitrogen and a fixed bed of the $\text{AlPO}_4\text{-5}$ at temperatures between 450 and 750°C in a flow reactor under 1 atm pressure. The goal of this study is to relate the conditions of the treatment to the resulting structure, composition, and chemical properties of the treated material.

EXPERIMENTAL

X-ray diffraction. XRD patterns were collected on a Rigaku diffractometer equipped with a Cu target and a Ni filter. The voltage was 35 kV at a filament current of 15 mA. The data of relative intensity were collected over a range of two- θ from 5 to 40° in step sizes of 0.02° at a rate of $10^\circ/\text{min}$.

Oxygen adsorption. The oxygen adsorption isotherms were determined in a static volumetric system of conventional design (4). Small samples (0.500 to 1.000 g) were degassed at 250°C under a pressure of 40 μTorr (1 Torr = 133.3 N/m^2) for 2 h. The sample was cooled to room temperature be-

fore it was immersed in a liquid nitrogen bath (ca. 77 K). The isotherm was developed by exposing the degassed sample to zero-grade oxygen (Air Products & Co.) under pressures to 100 Torr. The sample dead volume was determined using UHP helium (Air Products & Co.) as the non-sorbing gas. These data were fit to a three-term BET equation by use of the equation of state for the oxygen data,

$$(P + aP^2)V = nRT, \quad (1)$$

with $a = 6.6 \times 10^{-5} \text{ Torr}^{-1}$ for oxygen.

X-ray photoelectron spectra. XPS spectra were obtained on a Vacuum Generators Minilab III surface analysis system using Mg as the source at an energy of 1253.6 eV. Bremstrahlung radiation from this polychromatic source also excited the Auger transitions as well. All data were referenced to the carbon 1s line at 284.6 eV. Quantitative analyses were performed using the areas under the peaks of high resolution scans and the Schofield photoelectron cross-sections (10). Dr. J. S. Brinen (American Cyanamid Co., Stamford, CN) performed the XPS/Auger analyses.

Chemical analyses. Quantitative chemical analyses of all samples were performed by W. Katter of Applied Technical Services (Marietta, GA). Atomic absorption spectroscopy was used to determine the Si and Al content, whereas a wet technique was used for the P analysis. Qualitative chemical analyses by energy dispersive X-ray analysis was performed on the volatile residues from the quartz treatment reactor.

Silicon tetrachloride treatment. Dry nitrogen was saturated at room temperature with a single pass saturator containing the liquid silicon tetrachloride. The saturated gas was directed through a vertical quartz reactor containing 2 g of $\text{AlPO}_4\text{-5}$. A bypass of the saturator allowed for drying of the sample at 250°C for 2 h prior to contacting it with the saturated nitrogen. The quartz reactor was programmed at the desired rate ($5\text{--}25^\circ\text{C}/\text{min}$, or greater than $25^\circ\text{C}/\text{min}$) to the final temperature ($450\text{--}750^\circ\text{C}$) and then

held at the final temperature for 70, 120, or 180 min in the saturated nitrogen. The samples are identified in this paper by a three-element code (*T-R-D*) describing the reaction conditions. For example, a sample prepared by heating at a rate of $5^\circ\text{C}/\text{min}$ (*R*) from 250 to 450°C (*T*) and held at this temperature for 70 min (1.2 h, *D*) is designated as 450-5-1.2. Samples were cooled under dry N_2 and stored in a stoppered vial. Unlike earlier protocols (9), we did not wash the samples. Provisions were made for sampling volatile residues from the quartz reactor and analyzing the same by EDAX. The modified $\text{AlPO}_4\text{-5}$ samples retained their white color after the treatment with silicon tetrachloride.

Chemicals. $\text{AlPO}_4\text{-5}$ samples (Lots 13166-88 and 11790-68) were provided by Dr. E. M. Flanigen of Union Carbide (Tarrytown, NY). The SAPO-5 was synthesized in our laboratories by hydrothermal crystallization in the tri-*n*-propylamine (Pr_3N) system according to Example 13 of the SAPO patent (6). The pseudo-boehmite alumina (Catapal-B) was obtained from Vista Chemical and the tri-*n*-propylamine (Pr_3N) was secured from Alfa Chemicals. Orthophosphoric acid was obtained from Fisher Scientific Co. M-5 Cab-O-Sil (Cabot Corp.) was the source of silicon for the SAPO-5 preparation. Silicon tetrachloride was obtained from Aldrich Chemical Co.

Ammonia in helium was prepared by Matheson to have the following composition: 5.37 mol% ammonia and balance He. Pyridine from Aldrich Chemical Co. was purified by the freeze-pump-thaw technique in the vacuum system attached to the IR cell. Cumene, methanol, and toluene were used without further purification. The purities of these chemicals were checked by GC analysis. The nitrogen (UHP grade) carrier gases in the flow reaction were obtained from Air Products & Co.

H- and Na-mordenite were obtained from Dr. T. Thomas from the Georgia Tech Research Institute (Atlanta, GA). The Na-mordenite showed about 50–60% exchange

of the ions as determined from chemical analysis. Alumina obtained from Harshaw showed a BET surface area of $232 \text{ m}^2/\text{g}$ (11).

GC analysis. A Hewlett-Packard HP 5710A gas chromatograph equipped with a Valco sixport sample valve was used in the product analyses. This GC detected the peaks by flame ionization of the effluent from the 10-ft (1 ft = 0.3048 m) column ($\frac{1}{8}$ -in diameter) of GP 5% SP-1200/5% Bentone 34 on 100/120 mesh Supelcoport. The peaks were integrated with a HP 3380A recording integrator. The carrier gas flowrate was $20 \text{ cm}^3/\text{min}$. Different temperature programs were used for the toluene methylation and the cumene cracking reaction. The GC was programmed for the products of the toluene methylation as follows: initial temperature 75°C for 4 min, temperature-programmed at $8^\circ\text{C}/\text{min}$ to 130°C and held for 4 min. The temperature program for the cumene cracking reaction was isothermal at 110°C for 2 min, temperature program at $8^\circ\text{C}/\text{min}$ to 130°C and hold for 4 min.

Ammonia titration. The acid site density was determined gravimetrically in a Perkin-Elmer TGS-2 thermogravimetric analyzer described earlier (12). These samples were dehydrated by heating in UHP helium at 600°C for 1 h. The sample was cooled to the adsorption temperature under flowing He ($400 \text{ STP cm}^3/\text{min}$) and the weight recorded as the initial weight. The ammonia/He mixture was metered into the device with dry nitrogen in the proportions necessary to develop the desired partial pressure of ammonia at the sample. This adsorbate flow was continued for 2.5 h and then discontinued to allow the weakly bound ammonia to desorb in the He flow for 1.5 h. At the end of the purge the final weight was recorded. The mass of ammonia adsorbed is the difference between the initial and final weights. This procedure was repeated for several temperatures and ammonia partial pressures to develop isotherms and isobars.

IR of chemisorbed pyridine. The IR spec-

tra were recorded by equipment described previously (12). Samples (50 mg) were pressed into thin, transparent wafers about 0.5 in. (1 in. = 0.0254 m) in diameter. These wafers were evacuated to 1 μ Torr (1 Torr = 133.3 N/m²) for 4 h at 425°C. The sample was cooled in the vacuum, the blank IR spectrum of the catalysts recorded, and dosed with pyridine under prescribed pressures at the IR beam temperature. Pyridine exposures for 2–4 h were held at pressures of 1 to 7 Torr. The cell was evacuated at room temperature for 1 h and the IR spectra were recorded at the beam temperature.

Flow reactor. One reactor system was used for the cumene cracking and the toluene methylation reactions. A microreactor was constructed from quartz tubing (25-mm diameter \times 30 cm) affixed with an axial thermowell. This reactor was mounted vertically in a Lindberg furnace which was controlled by a Leeds and Northrup Electromax III temperature controller equipped with a type J thermocouple (iron-constantan). The carrier gas (UHP nitrogen) from two cylinders serviced the system. One stream, controlled by a rotameter, was the purge/diluent stream. The other was split and individually controlled by rotameters to saturators containing toluene and methanol. The methanol saturator was put in an ice bath, whereas the toluene saturator was at room temperature. The lines downstream of the saturator leading to the reactor were traced with electrical heating tape and maintained at 90°C. The reactor pressure was slightly above atmospheric pressure. The reactor effluent was traced with electrical heating tape and maintained at 150°C to prevent condensation in the lines. An in-line filter (7 μ m) in the reactor effluent prevented catalyst fines from entering the GC sample valve. For the cumene cracking reaction only one saturator was filled with cumene and it was held at room temperature. The classical tests for interparticle effects were negative for a bed of $\frac{1}{2}$ g or more; however, intraparticle tests showed that reaction rates over particles

equal to 100 μ m diameter were three times that for $\frac{1}{16}$ -in. extrudates. All catalysts were dried in N₂ at 500°C for 2 h prior to the probe reaction studies.

RESULTS AND DISCUSSION

Powder XRD of Samples

All samples were examined by powder XRD to determine crystallinity and cell constants. The silicon tetrachloride treatment produced crystalline samples at preparation temperatures between 450 to 750°C except for one sample prepared at 600°C (sample 600-5-3). One example of a material created at 450°C (sample 450-5-1.2, Fig. 1) is compared to the XRD of the parent AlPO₄-5. The positions of all peaks in the modified sample are very similar to those in the AlPO₄-5. These data were examined by the method of Cullity (13) to extract unit cell parameters (Table 1) for the hexagonal crystal. The 450°C samples show decreases in these parameters from the parent AlPO₄-5. For example, sample 450-5-1.2 shows a

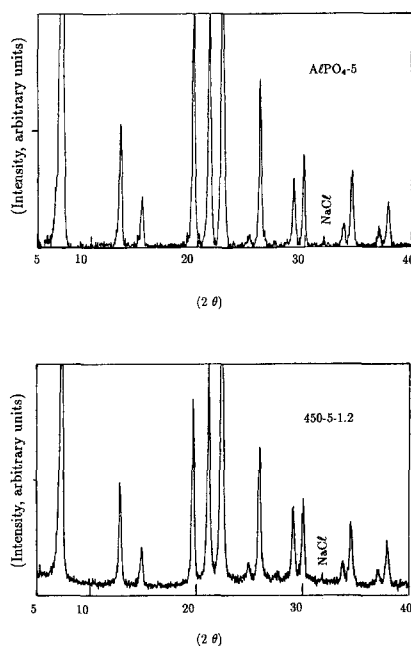


FIG. 1. X-ray diffraction spectra of AlPO₄-5 and modified AlPO₄-5.

TABLE I

Unit Cell Parameters for the Hexagonal System

| Sample | <i>a</i> (Å) | <i>c</i> (Å) |
|----------------------|---------------|--------------|
| AlPO ₄ -5 | 13.86 (13.73) | 8.41 (8.48) |
| SAPO-5 | 13.70 (13.60) | 8.47 (8.46) |
| 450-5-1.2 | 13.75 | 8.38 |
| 450-10-1.2 | ^a | ^a |
| 450-15-1.2 | 13.78 | 8.37 |
| 450-25-1.2 | 13.59 | 8.34 |
| 450-∞-1.2 | 13.69 | 8.36 |
| 550-5-1.2a | 13.75 | 8.38 |
| 550-5-1.2b | ^a | ^a |
| 600-5-1.2a | 13.75 | 8.40 |
| 600-5-1.2b | 13.75 | 8.41 |
| 600-5-2 | 13.79 | 8.41 |
| 600-5-3 | ^b | ^b |
| 750-5-1.2a | 13.79 | 8.40 |
| 750-5-1.2b | 13.68 | 8.38 |

Note. Literature values are shown in parentheses. Sources for these are Ref. (1) for AlPO₄-5 and Ref. (6) for SAPO-5.

^a Sample not indexed.

^b This sample showed broad XRD peaks and was not indexed.

decrease in the *a* parameter of 0.121 Å and a decrease in the *c* parameter of 0.027 Å. The materials prepared at higher temperatures show similar decreases in the unit cell parameters with the exception of 600-5-1.2b, which shows an increase in the *c* parameters and a decrease in the *a* parameter. The sample prepared at 600°C and 3 h (600-5-3) showed broad XRD peaks and was not indexed.

These XRD data suggest that the SiCl₄ treatment does not cause destruction of the crystal structure when the duration is limited to 1 h. Small changes in the unit cell parameters are observed for the modified samples relative to the parent AlPO₄; however, we are reluctant to explain these data by lattice contraction for the following reason. The unit cell constants of our standards (AlPO₄-5 and SAPO-5) differ from the literature values (≈ 0.1 Å) by the amount equal to that caused by the SiCl₄-treatment relative to the parent AlPO₄-5.

Bulk Chemical Composition

The chemical analyses of the samples (Table 2) are reported as mole fraction of metal ion in the formula Si_{*x*}Al_{*y*}P_{*z*}O₂. In this formula $x + y + z = 1.0$. The parent AlPO₄-5 material shows the expected composition, which is almost equimolar in Al₂O₃ and P₂O₅ but with very little silicon (1, 2). The SAPO-5 shows a Si/P/Al molar ratio of 1/2.77/3.37, which is different from that reported for a SAPO-37 (7).

Increasing the reaction temperature from 450 to 750°C results in materials having higher concentrations of silicon: $x = 0.036$ – 0.047 at 450°C to $x = 0.06$ – 0.1 for 750°C treatment; however, attempts to synthesize duplicate materials at fixed reaction conditions gave mixed results. At 450°C, the silicon content ($x = 0.04$) and ratio of Al₂O₃/P₂O₅ (1.02–1.04) were similar for nearly constant reaction conditions. The higher temperature treatments gave irreproducible silicon contents ($x = 0.065$ and 0.1) with similar Al₂O₃/P₂O₅ ratios (0.99 to 1.00) in the one case for reaction temperature at 750°C. The reaction at 600°C (600-5-1.2a,b) showed nearly similar silicon contents ($x = 0.061$, 0.067) but these samples gave different Al₂O₃/P₂O₅ ratios (0.88 and 0.98). The samples prepared at 600°C for 70, 120, and 180 min showed similar Si mole fractions. Thus, we cannot ascribe much significance to the effect of duration of reaction on the samples prepared at temperatures greater than 450°C. For the 450°C treatment we can ascribe some minor importance to the rate of programming upon the ultimate composition of the samples. At the lowest programming rate (5°C/min), the silicon content is less than what we observe at the higher programming rates (15 and 25°C/min).

We collected solid residues downstream of the treatment reactor which accumulated during the preparation of the following samples: 550°C (550-5-1.2a), 600°C (600-5-1.2a, -1.2b, -2), and 750°C (750-5-1.2a, -1.2b); these were analyzed by EDAX. The residues of the three samples prepared at 600°C

TABLE 2

Chemical Analyses, Oxygen Monolayer Volume, and Specific Conversion of Toluene over Catalysts

| Catalysts | Si _x | Al _y | P _z | O ₂ Volume ^a (STP cm ³ /g) | Toluene (%/g) ^b | Conversion ^c (%/STP cm ³) ^d |
|----------------------|-----------------|-----------------|----------------|--|-------------------------------|--|
| AlPO ₄ -5 | 0.002 | 0.494 | 0.504 | 80.79 | 3.25 | 0.04 |
| Na-Mordenite | | Si/Al = 10 | | — | 20.75 | — |
| SAPO-5 | 0.140 | 0.471 | 0.388 | 74.42 | 21.07 | 0.28 |
| H-Mordenite | | Si/Al = 10 | | 117.4 ^e | 35.01 | — |
| 450-5-1.2 | 0.036 | 0.489 | 0.475 | 82.17 | 12.34 | 0.15 |
| 450-10-1.2 | 0.045 | 0.482 | 0.473 | 76.14 | 9.80 | 0.13 |
| 450-15-1.2 | 0.047 | 0.481 | 0.472 | 77.19 | 17.14 | 0.22 |
| 450-25-1.2 | 0.045 | 0.486 | 0.469 | 71.92 | 9.44 | 0.13 |
| 450-∞-1.2 | 0.044 | 0.485 | 0.471 | 73.65 | 11.27 | 0.15 |
| 550-5-1.2a | 0.044 | 0.467 | 0.489 | — | 10.01 | — |
| 550-5-1.2b | 0.050 | 0.474 | 0.476 | 67.71 | 14.68 | 0.22 |
| 600-5-1.2a | 0.067 | 0.437 | 0.496 | 61.79 | 6.77 | 0.11 |
| 600-5-1.2b | 0.061 | 0.464 | 0.475 | 61.94 | 5.63 | 0.09 |
| 600-5-2.0 | 0.044 | 0.444 | 0.512 | 62.78 | 6.78 | 0.11 |
| 600-5-3.0 | 0.063 | 0.464 | 0.473 | 53.82 | 3.17 | 0.06 |
| 750-5-1.2a | 0.105 | 0.446 | 0.449 | 19.58 | 0.92 | 0.05 |
| 750-5-1.2b | 0.065 | 0.467 | 0.468 | 58.48 | 5.53 | 0.09 |

^a Monolayer volume extracted from data of O₂ uptake vs O₂ partial pressure fit to three-parameter BET equation.

^b Toluene conversion per gram of catalyst.

^c Reaction conditions: temperature, 425°C; weight hourly space velocity, 7.1 g of total liquid feed/h-g catalyst; toluene/methanol molar ratio, 2.5/1.0. Catalyst particle size is 100–200 mesh (≈100 μm).

^d Column 7 divided by column 5.

^e N₂ monolayer volume.

showed Al, P, and Cl, whereas the other samples showed only Al and Cl. Oxygen is not assayed by the instrument used in this study.

Oxygen Adsorption Isotherm at 77 K

The AlPO₄-5, SAPO-5, and the modified AlPOs were characterized by "oxygen filling" experiments at 77 K. The data were fit by the three-parameter BET technique (14) to extract monolayer volume in STP cm³ of gas/g of sample. A nonlinear fit of the adsorption data between the relative pressures of 0.0002 to 0.9 gave the monolayer volumes (Table 2). The AlPO₄-5 and SAPO-5 gave volumes of 80.8 and 74.4 STP cm³/g, respectively. The mild treatment at 450°C for the lowest programming rate produced a sample (450-5-1.2) having a volume of 82.2 STP cm³/g. Increasing the programming

rate to 10, 15, 25, and >25 C/min (indicated by ∞) produced samples having oxygen volumes of 76.1, 77.2, 71.9, and 73.7 STP cm³/g, respectively. These data suggest that the rate of temperature programming during the silicon tetrachloride has a small but significant effect of decreasing the pore volume of the samples. The pore volumes of the modified materials (450°C treatment) appear to be intermediate between the AlPO₄-5 parent material and the SAPO-5 sample.

The sample produced at 550°C (550-5-1.2) gave pore volumes of 67.7 STP cm³/g, whereas the samples synthesized at 600°C (600-5-1.2a, 600-5-1.2b, 600-5-2, and 600-5-3) showed pore volumes of 61.8, 61.9, 62.8, and 53.8 STP cm³/g. The two samples prepared at 750°C (750-5-1.2a,b) showed pore volumes of 19.6 and 58.5 STP cm³/g. In-

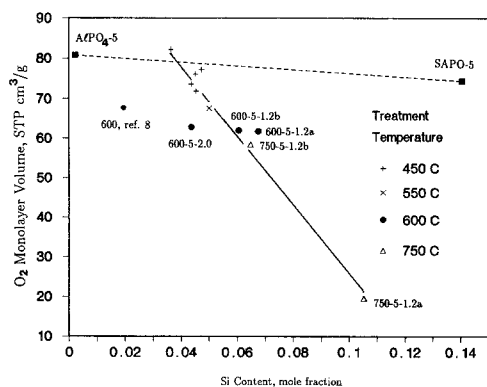


FIG. 2. Oxygen monolayer volume versus silicon content for samples treated in SiCl_4 .

creasing the temperature of the treatment apparently caused the pore volume to decrease. Moreover, the high-temperature treatments (greater than 600°C) gave irreproducible results in the observed pore volumes.

The data of oxygen filling were plotted versus silicon content (Fig. 2). The data for the 450°C materials fall on a line between the $\text{AlPO}_4\text{-5}$ and SAPO-5 materials, whereas the data for the other modified materials fall below this line. We speculate the materials synthesized at temperatures higher than 550°C may show pore blocking, perhaps by silicon. One literature datum (8) is plotted on this same figure at a silicon content near 0.02 and for a oxygen uptake of $68 \text{ STP cm}^3/\text{g}$. This point was calculated from the data of the nitrogen uptake for an $\text{AlPO}_4\text{-5}$ sample treated with SiCl_4 at 600°C . This treatment produced a 20% decrease in the nitrogen isotherm for the modified sample compared to the isotherm of the untreated $\text{AlPO}_4\text{-5}$. Thus, we represent this effect by plotting a point 20% below that of our starting material.

XPS and Auger Electron Spectroscopy

Samples were characterized by electron spectroscopy to develop XPS and Auger spectra. We chose the $\text{AlPO}_4\text{-5}$, SAPO-5 samples as standards to be compared to the materials prepared at 450 , 550 , 600 , and

750°C . The data of XPS binding energies for the Al, P, and Si $2p$ orbitals are reported in Table 3 with the Auger kinetic energies for the $\text{KL}_{23}\text{L}_{23}$ transitions. These data are used to create chemical state maps (Fig. 3) as described by Suib *et al.* (15) and Wagner *et al.* (16). The ordinate of the chemical state is the kinetic energy of the Auger transition, whereas the abscissa is the XPS binding energy. In addition we shall exam-

TABLE 3

Photoelectron and Auger Transitions for the SiCl_4 -Treated Materials

| Sample | Transition | Binding energy (eV) | Kinetic energy (eV) | Modified Auger parameter (eV) |
|--------------------------|----------------------------------|---------------------|---------------------|-------------------------------|
| $\text{AlPO}_4\text{-5}$ | Al ($2p$) | 75.2 | | |
| | P ($2p$) | 135.1 | | |
| | Al $\text{KL}_{23}\text{L}_{23}$ | | 1385.4 | 1460.6 |
| | P $\text{KL}_{23}\text{L}_{23}$ | | 1847.8 | 1982.9 |
| SAPO-5 | Al ($2p$) | 75.6 | | |
| | Si ($2p$) | 102.8 | | |
| | P ($2p$) | 134.9 | | |
| | Al $\text{KL}_{23}\text{L}_{23}$ | | 1385.7 | 1461.3 |
| | Si $\text{KL}_{23}\text{L}_{23}$ | | 1608.7 | 1711.5 |
| 450-5-1.2 | Al ($2p$) | 75.5 | | |
| | Si ($2p$) | 102.5 | | |
| | P ($2p$) | 135.0 | | |
| | Al $\text{KL}_{23}\text{L}_{23}$ | | 1385.0 | 1460.5 |
| 450-15-1.2 | Al ($2p$) | 75.7 | | |
| | Si ($2p$) | 102.9 | | |
| | P ($2p$) | 135 | | |
| | Al $\text{KL}_{23}\text{L}_{23}$ | | 1385.0 | 1460.7 |
| 550-5-1.2a | Al ($2p$) | 75.8 | | |
| | Si ($2p$) | 103.4 | | |
| | P ($2p$) | 135.0 | | |
| | Al $\text{KL}_{23}\text{L}_{23}$ | | 1384.6 | 1460.4 |
| 600-5-1.2a | Al ($2p$) | 75.6 | | |
| | Si ($2p$) | 103 | | |
| | P ($2p$) | 134.8 | | |
| | Al $\text{KL}_{23}\text{L}_{23}$ | | 1384.9 | 1460.5 |
| 750-5-1.2b | Al ($2p$) | 75.9 | | |
| | Si ($2p$) | 103.8 | | |
| | P ($2p$) | 135.4 | | |
| | Al $\text{KL}_{23}\text{L}_{23}$ | | 1385.0 | 1460.9 |
| SAPO-5 | Al ($2p$) | 75.6 | | |
| | Si ($2p$) | 102.8 | | |
| | P ($2p$) | 134.9 | | |
| | Al $\text{KL}_{23}\text{L}_{23}$ | | 1385.7 | 1461.3 |
| 600-5-1.2a | Al ($2p$) | 75.6 | | |
| | Si ($2p$) | 103 | | |
| | P ($2p$) | 134.8 | | |
| | Al $\text{KL}_{23}\text{L}_{23}$ | | 1384.9 | 1460.5 |
| 750-5-1.2b | Al ($2p$) | 75.9 | | |
| | Si ($2p$) | 103.8 | | |
| | P ($2p$) | 135.4 | | |
| | Al $\text{KL}_{23}\text{L}_{23}$ | | 1385.0 | 1460.9 |
| SAPO-5 | Al ($2p$) | 75.6 | | |
| | Si ($2p$) | 102.8 | | |
| | P ($2p$) | 134.9 | | |
| | Al $\text{KL}_{23}\text{L}_{23}$ | | 1385.7 | 1461.3 |
| 600-5-1.2a | Al ($2p$) | 75.6 | | |
| | Si ($2p$) | 103 | | |
| | P ($2p$) | 134.8 | | |
| | Al $\text{KL}_{23}\text{L}_{23}$ | | 1384.9 | 1460.5 |
| 750-5-1.2b | Al ($2p$) | 75.9 | | |
| | Si ($2p$) | 103.8 | | |
| | P ($2p$) | 135.4 | | |
| | Al $\text{KL}_{23}\text{L}_{23}$ | | 1385.0 | 1460.9 |
| SAPO-5 | Al ($2p$) | 75.6 | | |
| | Si ($2p$) | 102.8 | | |
| | P ($2p$) | 134.9 | | |
| | Al $\text{KL}_{23}\text{L}_{23}$ | | 1385.7 | 1461.3 |
| 600-5-1.2a | Al ($2p$) | 75.6 | | |
| | Si ($2p$) | 103 | | |
| | P ($2p$) | 134.8 | | |
| | Al $\text{KL}_{23}\text{L}_{23}$ | | 1384.9 | 1460.5 |
| 750-5-1.2b | Al ($2p$) | 75.9 | | |
| | Si ($2p$) | 103.8 | | |
| | P ($2p$) | 135.4 | | |
| | Al $\text{KL}_{23}\text{L}_{23}$ | | 1385.0 | 1460.9 |

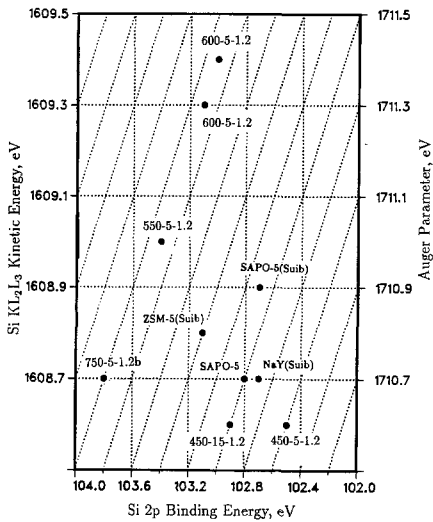


Fig. 3. Chemical state plot of silicon in modified $\text{AlPO}_4\text{-5}$ and standards.

ine the XPS data to describe the chemical composition of the surface region.

The chemical state of silicon (Fig. 3) in materials prepared at 450°C is similar to the chemical state of Si in SAPO-5 prepared from primary synthesis. On this same figure we have included the data of Suib *et al.* (15) and Wagner *et al.* (16) for SAPO-5, ZSM-5, and Na-Y. However, the samples prepared at 550 , 600 , and 750°C show a chemical state for silicon which is different from that of the 450°C materials and the SAPO-5. A useful parameter for evaluating the gross

chemical state of the element is the modified Auger parameter, which is the sum of the ordinate and abscissa values in Fig. 3. The Auger parameters for the materials prepared at 550°C and higher show values of $1712.4\text{--}1712.5$ eV, which are about 1 eV greater than that for the 450°C materials ($1711.1\text{--}1711.5$ eV). The sample of ZSM-5 having a high silica–alumina ratio (180) shows an Auger parameter of 1711.9 eV, which is similar to that for the samples prepared at 550°C and above.

The chemical state plots for aluminum and phosphorus show very little difference between the samples. The Auger parameters for these materials differ by $0.4\text{--}0.5$ eV with no apparent trend in response to increasing temperatures. These data suggest that the SiCl_4 treatment affected only a small portion of the Al and P ions. All of the modified materials show chemical states for aluminum which are different from that of alumina. For example, the modified Auger parameter for alumina is at least 1 eV higher than the modified sample prepared at 750°C .

The surface and chemical compositions are summarized in Table 4 for the $\text{AlPO}_4\text{-5}$ and SAPO-5 standards plus the materials prepared at 450 , 600 , and 750°C . The surface and bulk compositions agree for the $\text{AlPO}_4\text{-5}$ standard; however, the SAPO-5 standard shows an Al/P ratio which is higher in the surface region (1.8) than in the bulk

TABLE 4
Surface and Bulk Composition of Standards and Modified Materials

| Sample | Bulk analysis | | | Surface analysis | | |
|--------------------------|---------------|--------------|-------|------------------|-------------|-------|
| | Al/P | Si/Al | Si/P | Al/P | Si/Al | Si/P |
| $\text{AlPO}_4\text{-5}$ | 0.98 (0.99) | 0.004 | 0.004 | 0.99 (1.10) | 0.001 | 0.001 |
| SAPO-5 | 1.22 (1.04) | 0.297 (0.17) | 0.362 | 1.75 (1.80) | 0.55 (0.39) | 0.96 |
| 450-5-1.2 | 1.03 | 0.074 | 0.076 | 1.0 | 0.021 | 0.021 |
| 450-15-1.2 | 1.02 | 0.098 | 0.100 | 1.00 | 0.057 | 0.057 |
| 600-5-1.2a | 0.88 | 0.153 | 0.135 | 1.02 | 0.043 | 0.044 |
| 750-5-1.2b | 1.00 | 0.139 | 0.139 | 1.08 | 0.103 | 0.111 |

Note. Values in parentheses are from Ref. (15).

(1.2). The modified samples all show a surface composition ratio of Si/Al which is less than the bulk ratio of Si/Al. The surface Si/P ratio is also smaller than the bulk Si/P ratio for the modified materials. The surface and bulk Al/P ratios are similar for the modified materials.

The XPS/Auger data confirm the presence of silicon in the AIPO₄-5 samples modified by the silicon tetrachloride treatment. None of the surface analyses showed Cl, which suggests that no AlCl₃ or PCl₅ remains in the samples. These modified samples show surface Si/Al and Si/P ratios which are smaller than the bulk.

Others have reported similar results for Y zeolites dealuminated by reaction with silicon tetrachloride (17, 18). They explained the nonuniform distribution of Si/Al in the samples by a model showing aluminum-rich exteriors. The authors speculated that the aluminum was redeposited near the external surface of crystals (17) as a result of the highly exothermic reaction of silicon tetrachloride which produced interiors hotter than the exterior of the crystals. Thus, the volatile aluminum compounds (perhaps aluminum chloride which sublimates at 181°C (19)) migrated to the cooler parts of the zeolite crystals. We suggest that the same model can explain our results for samples which are rich in Al and P at the surface.

In the case of phosphorus, the volatile species may be the oxides (perhaps P₄O₁₀ which sublimates at 360°C) since PCl₅ decomposes at 160°C (19). Qualitative analyses of residue downstream of the treatment vessel showed Al and P species, which confirms their volatility under reaction conditions. Moreover, since the only source of Al and P is the AIPO₄-5 we conclude that the treatment "extracted" them from the AIPO₄-5.

The XPS data shed light on the nature of the material occluding the pores of the materials prepared at temperatures higher than 450°C. The silicon XPS/AES data show that the materials prepared at 450°C have a chemical state very similar to that of the Si

in SAPO-5 reference and the SAPO-5 reported by Suib *et al.* (15). However, the materials prepared at 550°C and above show a chemical state which is closer to the Si in a silicon-rich ZSM-5 sample. We interpret these data by a model for which the Si is "isolated" from neighboring Si in the samples prepared at 450°C. However, the samples prepared at higher temperatures show a Si environment rich with Si neighbors. We conclude that the materials prepared at 550°C and higher show silicon-rich oxides blocking the pores.

Ammonia Titration, IR Spectra, Probe Reactions

Ammonia titration. Ammonia isobars at 10 Torr (Fig. 4) were developed to determine that temperature which allowed the best discrimination among the modified catalysts. These data show that ammonia sorption at 150°C and 10 Torr can be used to discriminate between several of the modified materials and the AIPO₄-5 and SAPO-5 standards. Temperatures higher than 150°C produced an isobar at 10 Torr showing smaller differences between the catalysts. The isotherm at 75°C showed very little difference between the AIPO₄-5 and SAPO-5 standards and the monolayer amounts of

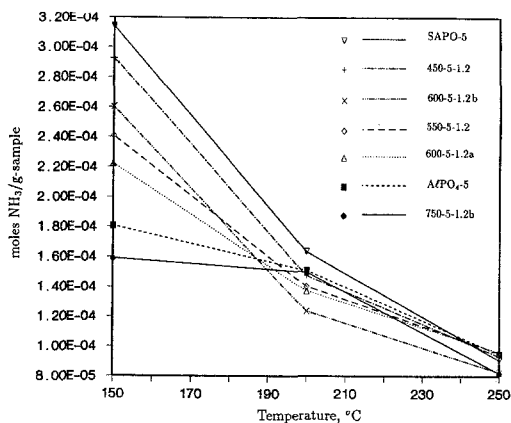


FIG. 4. Ammonia isobars for AIPO₄-5, SAPO-5, and modified AIPO₄-5.

ammonia chemisorbed at 75°C (1.35 and 1.51×10^{-3} mol/g catalysts, respectively) are about eight times that chemisorbed at 150°C and 10 Torr. All of the acidity titrations at 150°C and 10 Torr ammonia are given in Table 5.

The materials prepared at 450°C show specific ammonia retentions at 150°C near $2.9\text{--}3.3 \times 10^{-4}$ mol/g catalysts, which is nearly twice that of the parent $\text{AlPO}_4\text{-5}$ (1.80×10^{-4} mol/g) and similar to the ammonia retention of SAPO-5 (3.15×10^{-4} mol/g). The modified materials prepared at 550 and 600°C show retentions of $2.2\text{--}2.6 \times 10^{-4}$ mol/g; whereas, the material prepared at 750°C shows ammonia pickup (1.65×10^{-4} mol/g) less than that of the $\text{AlPO}_4\text{-5}$.

The modified $\text{AlPO}_4\text{-5}$ samples retain different amounts of ammonia according to the preparation temperature. The retention depends partly upon the available surface area as determined by oxygen filling. The ammonia retention data were ratioed to the

oxygen monolayer volume to account for surface area effects (Table 5). These data show that the modified materials have higher affinity for ammonia than the untreated $\text{AlPO}_4\text{-5}$ ($3.4\text{--}4.4 \times 10^{-6}$ mol ammonia/STP cm^3 of O_2 vs 2.2×10^{-6}). Only the sample prepared at 750°C showed a specific ammonia retention which was less than the others (2.8×10^{-6} vs $3.8\text{--}4.4 \times 10^{-6}$ mol ammonia/STP cm^3). Apparently, the materials prepared at temperatures lower than 750°C have similar surface affinities for the ammonia titre. Moreover, the materials prepared at 450°C show ammonia affinities ($3.6\text{--}4.4 \times 10^{-6}$ mol NH_3 /STP cm^3) similar to that for SAPO-5 (4.2×10^{-6} mol ammonia/STP cm^3).

IR spectra of chemisorbed pyridine. Pyridine was used to describe the type of acidities present on the surface of the catalysts. We calibrated our apparatus for the pyridine IR spectra over standards of alumina (Lewis acid), H-mordenite (Brønsted and Lewis acids), and silica (hydrogen-bonded pyridine). Lewis-bound pyridine on alumina shows a peak at 1490 cm^{-1} and three peaks at 1610, 1590, and 1575 cm^{-1} . One other peak is obvious at 1445 cm^{-1} . The pyridinium ion present on pyridine/H-mordenite shows a distinctive IR pattern with a peak at 1540 cm^{-1} , whereas this peak is absent in samples without Brønsted sites (i.e., no pyridinium ion). Other peaks are present at 1490, 1450, and 1590 cm^{-1} . The IR spectrum of pyridine which is hydrogen-bonded to the surface of silica shows only two peaks: 1595 and 1445 cm^{-1} . The calibration standards allow us to interpret the IR spectra of pyridine sorbed to model catalysts.

The IR spectra (Fig. 5a) of pyridine sorbed to $\text{AlPO}_4\text{-5}$ shows peaks at 1610, 1490, and 1450 cm^{-1} . A shoulder at 1440 cm^{-1} is present in the sample for low pyridine exposure pressure (1.1 Torr). The SAPO-5 samples (Fig. 5b) shows relaxations at 1610, 1540, 1490, 1450, and 1440 cm^{-1} at a pyridine exposure of 1.01 Torr. A sample prepared at 450°C in silicon tetrachloride shows strong peaks at 1610, 1490,

TABLE 5

Ammonia Titrations for Standard and Modified Catalysts

| Catalysts | Ammonia adsorbed ^a mol/g catalyst $\times 10^{+4}$ | Ammonia ^b / oxygen volume $\times 10^{-6}$ |
|--------------------------|---|---|
| $\text{AlPO}_4\text{-5}$ | 1.80 | 2.23 |
| 450-5-1.2 | 2.95 | 3.59 |
| 450-10-1.2 | 3.05 | 4.01 |
| 450-15-1.2 | 3.30 | 4.28 |
| 450-25-1.2 | 3.18 | 4.42 |
| 450-∞-1.2 | 2.85 | 3.87 |
| 550-5-1.2a | 2.41 | — |
| 550-5-1.2b | 2.28 | 3.37 |
| 600-5-1.2a | 2.22 | 3.59 |
| 600-5-1.2b | 2.61 | 4.21 |
| 750-5-1.2b | 1.65 | 2.82 |
| SAPO-5 | 3.15 | 4.23 |

^a Temperature, 150°C; ammonia partial pressure, 10 Torr; values in columns are moles ammonia retained after inert purge at 150°C.

^b Ratio of values in column 2 to O_2 monolayer volumes (Table 2, column 5); units are mol NH_3 /STP cm^3 of O_2 .

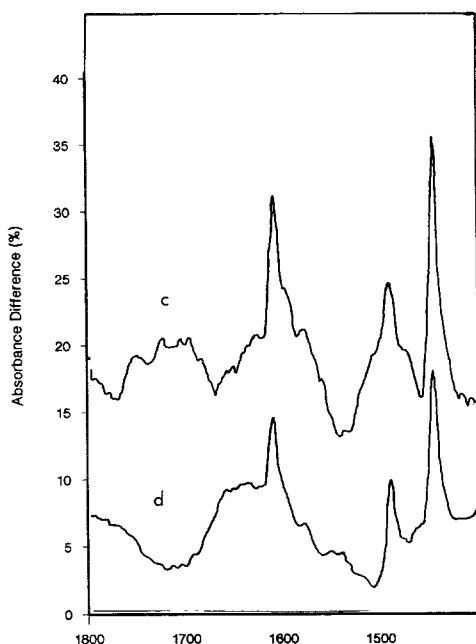
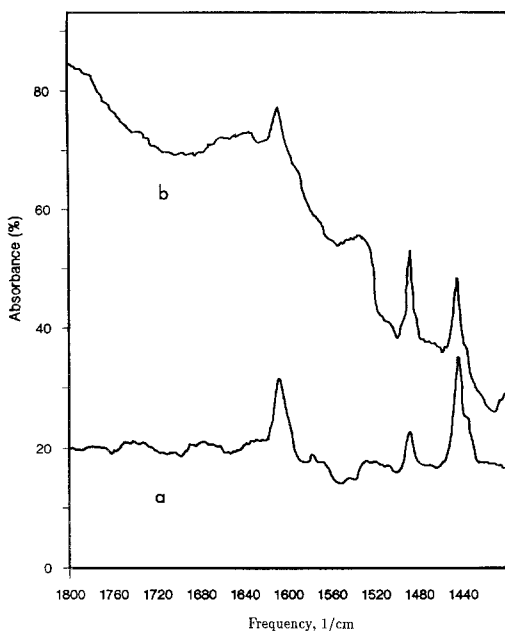


FIG. 5. Infrared spectra of pyridine chemisorbed to $\text{AlPO}_4\text{-5}$, SAPO-5, and modified $\text{AlPO}_4\text{-5}$. (a) $\text{AlPO}_4\text{-5}$; (b) SAPO-5; (c) 450-5-1.2; (d) 600-5-1.2.

and 1440 cm^{-1} with a shoulder peak at 1575 cm^{-1} at pyridine pressures of 0.80 Torr (Fig. 5c). No peaks are evident at 1540

cm^{-1} . These same peaks are evident for the sample prepared at 600°C (Fig. 5d) for a pyridine pressure of 2.05 Torr.

Toluene methylation activity. The results of preliminary studies indicated that the following conditions were appropriate: temperature = 425°C ; toluene/methanol feed ratio (molar) = 2.5/1.0; weight hourly space velocity = 7.1 g of total liquid feed/h-g catalyst. Under these conditions we could discriminate between the activities of the $\text{AlPO}_4\text{-5}$, SAPO-5, modified $\text{AlPO}_4\text{-5}$ samples, and mordenites. The catalyst activity decreased with time on stream (1–2% after 2 h) so that we report here initial rates. On the basis of published data for *n*-butane cracking (20, 21), the $\text{AlPO}_4\text{-5}$ reference catalyst was expected to show low alkylation activity relative to H-mordenite. We confirmed these findings in our initial tests.

Several molecular sieve catalysts were evaluated to provide an understanding for the response of the toluene alkylation activity/selectivity to changes in surface acidity. The H-mordenite and Na-mordenite catalyst document the effects of changing Brønsted acidity upon the alkylation activity/selectivity.

The $\text{AlPO}_4\text{-5}$ and SAPO-5 catalyst define the effects of changing Si content between isostructural samples. The activity/selectivity trends for these "standards" provide guidance for interpreting the alkylation data of the modified $\text{AlPO}_4\text{-5}$ samples.

The specific conversion of toluene over these standards and the modified $\text{AlPO}_4\text{-5}$ samples are given in Table 2. The $\text{AlPO}_4\text{-5}$ shows low specific conversion of the toluene (3.25%/g catalyst) under the conditions where the SAPO-5 (21.07%/g), Na-mordenite (20.75%/g), and H-mordenite (35.01%/g) show higher conversions. The $\text{AlPO}_4\text{-5}$ modified at 450 and 550°C shows specific conversions of 9.4 to 17.1%/g, whereas the materials prepared at higher temperatures show conversions which are less than 7%/g. Apparently the temperature of the silicon tetrachloride affects the cata-

lytic properties of the catalysts and all but two of the modified materials are more active than the parent $\text{AlPO}_4\text{-5}$.

The $\text{AlPO}_4\text{-5}$ zeolite shows only xylenes as the products with *ortho* (0.51), *para* (0.27) isomers as the favored products and with *meta* xylene as the minority product (0.22). The SAPO-5 also showed xylenes but with equal amounts of *meta* and *ortho* isomers (0.38) and less *para* isomer (0.24). All modified materials showed xylene distributions similar to that for 450-5-1.2 for which the *ortho*, *o*, isomer predominates (0.51); *para*, *p* (0.27), and *meta*, *m* (0.22), occur in smaller amounts. The H-mordenite shows a xylene distribution (*o/p/m* = 0.26/0.23/0.51) not unlike that predicted from equilibrium thermodynamics under reaction conditions (*o/p/m* = 0.25/0.23/0.52). The Na-mordenite showed a xylene distribution similar to that observed from the SAPO-5 catalyst (*o/p/m* = 0.42/0.19/0.39).

No ethyl benzene or styrene was observed as products from any of the catalysts we tested. Ethyl benzene and styrene were injected into the feed under reaction conditions and we observed less than 5% conversion of the ethyl benzene and only 12% conversion of the styrene for the Na-mordenite catalyst under the reaction conditions.

Cumene cracking reaction. The Brønsted acidities of the standard and modified catalysts were tested by the activity of the cumene cracking reaction at temperatures between 300 and 500°C at a weight hourly space velocity of 6.5 g/h-g catalysts. Pseudo-first-order rate constants were determined at each temperature and we report here the constants at 400°C (Table 6). The trends shown for the 400°C data truly reflect the results from the tests at the other temperatures. The modified materials all show low cracking rate constants (20–150 $\text{cm}^3/\text{g}\cdot\text{min}$) similar to that observed for the parent $\text{AlPO}_4\text{-5}$ (57.5 $\text{cm}^3/\text{g}\cdot\text{min}$) but much lower than the SAPO-5 activity (447 $\text{cm}^3/\text{g}\cdot\text{min}$).

The cumene cracking activity (1388 $\text{cm}^3/$

TABLE 6

| Cumene Rate Constants at 400°C | |
|--------------------------------|--|
| Sample | k ($\text{cm}^3/\text{g}\cdot\text{min}$) ^a |
| $\text{AlPO}_4\text{-5}$ | 57.5 |
| Na-mordenite | 304.5 |
| SAPO-5 | 446.7 |
| H-mordenite | 1388. |
| 450-5-1.2 | 147.6 |
| 450-10-1.2 | 58.5 |
| 450-15-1.2 | 39.8 |
| 450-∞-1.2 | 72.7 |
| 550-5-1.2b | 51.5 |
| 600-5-1.2a | 45.8 |
| 600-5-1.2b | 81.3 |
| 600-5-2 | 22.7 |
| 600-5-3 | 58.8 |
| 750-5-1.2b | 20.1 |

^a Reaction conditions: temperature, 400°C; liquid weight hourly space velocity, 6.5 g cumene/h-g catalyst. Catalyst particle size 120–200 mesh ($\approx 100 \mu\text{m}$). Catalyst was dehydrated in N_2 at 500°C for 2 h. Data of conversion were reduced assuming first-order kinetics to give pseudo-first-order rate constants having units of $\text{cm}^3/\text{g}\cdot\text{min}$. Bed density data (g/cm^3 of bed) are required to produce a first-order rate constant having units of reciprocal time.

g-min) of a reputed Brønsted acid, H-mordenite, is 24 times that of the $\text{AlPO}_4\text{-5}$. A partially exchanged mordenite (Na-mordenite, about 50–60% exchanged) shows a cumene cracking activity less than the SAPO-5 (305 vs 447 $\text{cm}^3/\text{g}\cdot\text{min}$) and much less than the H-mordenite.

The acid sites present on the modified materials show Lewis acidity as indicated by the pyridine IR spectra, whereas the SAPO-5 standard shows both Lewis and Brønsted acidity. The cumene cracking data confirm the absence of strong Brønsted sites in the $\text{AlPO}_4\text{-5}$ and modified materials, whereas SAPO-5 shows Brønsted sites similar to those remaining in a partially exchanged Na-mordenite. These results for the $\text{AlPO}_4\text{-5}$ are different from those reported by Choudhary and Akolekar

(22). They report Brønsted acidity in $\text{AlPO}_4\text{-5}$ for the cracking of cumene and isomerization of *o*-xylene. However, the activity of these catalysts decreased rapidly with increasing pulses of reactant in the micro-reactor. Such transient effects may not be observed in our continuous flow reactor.

None of the modified materials showed any activity for the base-catalyzed alkylation of methanol to the toluene side chain to form ethyl benzene; however, the selectivity to form xylenes did confirm the presence of acid sites. As expected, the modified materials were more active than the untreated $\text{AlPO}_4\text{-5}$ for the methylation reaction. Moreover, the *ortho*, *para* selectivity of the modified samples is similar to that observed over Friedel-Crafts catalysts (23), which suggests that only Lewis acid sites are present as confirmed by the pyridine IR spectra of the same samples. Brønsted sites are known to isomerize *ortho* xylene in a manner that is predicted from equilibrium thermodynamics (24, 25). We confirmed this finding with the methylation reaction over the H-mordenite, which showed high activity to toluene conversion and equilibrium distribution of the xylenes. Selective positioning of the Brønsted sites by ion exchange with sodium reduces the activity of the catalysts and shifts the xylene distribution away from the *meta*-favored selectivity predicted by equilibrium thermodynamics. The similar methylation activity/selectivity of the SAPO-5 to the Na-mordenite suggests that weak Brønsted sites are present in the SAPO-5 but are absent in the materials modified by silicon tetrachloride. Indeed, the cumene cracking activities were similar for the SAPO-5 and Na-mordenite.

The toluene methylation activity apparently depended upon total surface area in a manner similar to that observed for the ammonia pickup. We plotted the specific toluene conversion vs oxygen monolayer volume (Fig. 6) to test this hypothesis. Indeed, the toluene conversion did increase for increasing oxygen volume of the modified materials. The catalytic activities of these

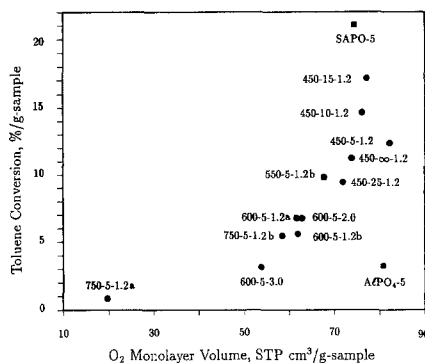


Fig. 6. Toluene methylation activity versus oxygen monolayer volume.

materials approached that of the SAPO-5 standard and they were distinctly different from the $\text{AlPO}_4\text{-5}$ starting material. We analyze these same data by ratioing the specific conversion to the specific monolayer volume (Table 2) to give the percentage toluene conversion per STP cubic centimeter. These data indicate significant increase in area-specific activity for treating the $\text{AlPO}_4\text{-5}$ with silicon tetrachloride. The materials prepared at 450 to 550°C showed area-specific activities of 0.13 to 0.22%/STP cm^3 , whereas the $\text{AlPO}_4\text{-5}$ showed area-specific activity of 0.04%/STP cm^3 . The materials prepared for long durations (2–3 h) at 600 and at 750°C showed activities less than or equal to 0.11%/ cm^3 .

As a final check of the Lewis acid catalysis in these catalysts we plotted the specific toluene conversion versus the specific ammonia retention (Fig. 7). If the reaction is catalyzed chiefly by Lewis sites, then the activity should correlate with the acid site density determined from the ammonia titration. Indeed, the data of conversion do correlate with ammonia chemisorption. The cumene cracking rate constants show little change for increasing amounts of ammonia retention. Thus, we conclude, that the ammonia retention is a measure of the Lewis acidity in the samples. Moreover, the amount of Brønsted acidity is small and constant in the samples we tested.

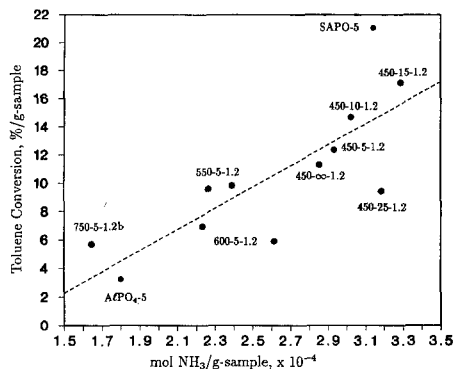


FIG. 7. Toluene methylation activity versus ammonia site density.

CONCLUSIONS

We believe that the silicon tetrachloride treatment changes the $\text{AlPO}_4\text{-5}$, rendering it more active for the toluene methylation reaction than the untreated $\text{AlPO}_4\text{-5}$. None of the modified samples catalyzed the side chain alkylation reaction to form ethyl benzene and styrene. Apparently treatments at 450 to 600°C alter the total surface area without seriously affecting the intrinsic chemistry. The more severe treatments (750°C) leave a silicon-rich residue in the pores which decreases the observed reaction rate and ammonia retention.

The role of silicon in the toluene methylation catalysis is not clear. The definitive structural tests for silicon incorporation (^{29}Si MAS-NMR) were inconclusive; thus we cannot determine the position of the Si ions in the modified materials (4). The silicon in SAPO-5 may play a role in creating Brønsted acidity as evident from the cumene cracking activity of this sample. However, the silicon obviously does not play the same role in the modified materials as confirmed by the low cumene cracking activities of these samples. We speculate that the silicon tetrachloride treatment creates a surface having only Lewis acidity. Attempts to add water back to the modified samples do not create strong Brønsted sites as determined by pyridine IR spectra although water is sorbed (4). Thus, the effect

of the silicon tetrachloride may produce a surface which cannot activate water to form protons as has been observed on other Brønsted acids which have been thoroughly dehydrated (24–26).

Some of the data appear to conflict; that is, the XPS of the 450°C-treated samples show a Si environment not unlike that of the Si in SAPO-5, but these same samples produce surfaces which show only Lewis acidity. We may resolve these conflicting data by one or both of the following hypotheses: (1) multiple layers of silicon ions are present even for the samples prepared at 450°C or (2) pairs of Si are inserted for Al, P ions. The lower layer of silicon ions which have neighbors other than silicon (e.g., Al, and P) produces the XPS data which are similar to those of the silicon in SAPO-5. The upper layer(s) of silicon ions covers the lower layers such that no Brønsted acidity is apparent. The number of layers present increases with Si content, which is suggested by the change in the chemical state of the Si toward a silicon-rich environment. We suggest that the pore volume decreases as a result of pore filling by layers of silicon-rich oxide. For the alternate hypothesis, the pair of silicons substituting for Al, P will not create a charge imbalance; thus no protons will be necessary to balance the charge and no Brønsted acidity is generated.

Phosphorus need not be present in the sample for it to catalyze the methylation reaction as the H- and Na-mordenites are active. Since Al is present in the modified $\text{AlPO}_4\text{-5}$, SAPO-5, and the aluminosilicates, we believe that it plays a role in the methylation catalysis. Aluminium has been used as an efficient alkylation catalyst as AlCl_3 (27) and as an oxide it shows Lewis acidity (24–26). Thus, its role as a participant in the methylation reaction is not surprising.

ACKNOWLEDGMENTS

We gratefully acknowledge the discussions with Dr. Tudor Thomas and Dr. Rosemarie Szostak of the Georgia Tech Research Institute, Atlanta, Georgia.

The authors thank Dr. E. M. Flanigen (Union Carbide) for the AIPO₄-5 samples and Dr. J. S. Brinen (American Cyanamid) for performing the electron spectroscopy analyses.

REFERENCES

1. Wilson, S. T., Lok, B. M., and Flanigen, E. M. US Patent 4,310,440 (1982).
2. Wilson, S. T., Lok, B. M., Messina, C. A., Cannan, T. R., and Flanigen, E. M., *J. Amer. Chem. Soc.* **104**, 1146 (1982); *ACS Symp. Ser.* **218**, 79 (1983).
3. Bennett, J. M., Cohen, J. P., Flanigen, E. M., Gluth, J. J., and Smith, J. V., *ACS Symp. Ser.* **218**, 109 (1983).
4. Brinen, J. L., PhD thesis, Georgia Institute of Technology, Atlanta, GA (1989).
5. Lok, B. M., Messina, C. A., Patton, R. L., Gajek, R. T., Cannan, T. R., and Flanigen, E. M., *J. Amer. Chem. Soc.* **106**, 6093 (1984).
6. Lok, B. M., Messina, C. A., Patton, R. L., Gajek, R. T., Cannan, T. R., and Flanigen, E. M., US Patent 4,440,871 (1984).
7. Saldarriaga, L. S., Saldarriaga, C., and Davis, M. E., *J. Amer. Chem. Soc.* **109**, 2686 (1987).
8. Theocharis, C. R., and Gelsthorpe, M. R., "Characterization of Porous Solids" (K. K. Unger *et al.*, Eds.), pp. 541–546. Elsevier Science, B. V. Amsterdam, Netherlands, 1988.
9. Beyer, H. K., and Belenykaja, I., "Catalysis by Zeolites" (Imelik *et al.*, Eds.), pp. 203–210. Elsevier Science, B. V. Amsterdam, Netherlands, 1980; Anderson, J. R., Chang, Y. F., and Hughes, A. E., *Catal. Lett.* **2**, 279–286 (1989); Sulikowski, B., Borbely, G., Beyer, H. K., Karge, H., and Mishin, I. W., *J. Phys. Chem.* **93**, 3240–3243 (1989).
10. Barr, T. L., in "Practical Surface Analysis by Auger and X-Ray Photoelectron Spectroscopy" (D. Briggs and M. P. Seah, Eds.). Wiley, New York, 1983.
11. Rosenthal, D. J., White, M. G., and Parks, G. D., *AIChE J.* **33**(2), 236 (1987).
12. Babb, K. H., and White, M. G., *J. Catal.* **98**, 343 (1986).
13. Cullity, B. D., "Elements of X-Ray Diffraction," 2nd ed. Addison-Wesley, Reading, MA, 1978.
14. Brunauer, S., Deming, L. S., Deming, W. E., and Teller, E., *J. Amer. Chem. Soc.* **62**, 1723–1732 (1940).
15. Suib, S. L., Winiiecki, A. M., and Kostapapas, A., *Langmuir* **3**(4), 483–488 (1987).
16. Wagner, C. D., Gale, L. M., and Raymond, R. M., *Anal. Chem.* **51**, 466–482 (1979).
17. Arribas, J., Corma, A., Fornes, V., and Melo, F., *J. Catal.* **108**, 135 (1987).
18. Dwyer, J., Fitch, F. R., Quin, G., and Vickerman, J. C., *J. Phys. Chem.* **86**, 4574 (1982).
19. Dean, J. A., Ed., "Lange's Handbook of Chemistry," 12th ed. McGraw-Hill, New York, 1979.
20. Flanigen, E. M., Lok, B. M., Patton, R. L., and Wilson, S. T., in "New Developments in Zeolite Science and Technology" (Y. Murakami, A. Iijima, and J. W. Ward, Eds.), pp. 103–112. Elsevier, Amsterdam, 1986.
21. Flanigen, E. M., Lok, B. M., Patton, R. L., and Wilson, S. T., *Pure Appl. Chem.* **58**, 1351, 1358 (1986).
22. Choudhary, V. R., Akolekar, D. B., Singh, A. P., and Sansare, S. D., *J. Catal.* **111**, 255 (1987).
23. Allen, R. H., and Yats, L. D., *J. Amer. Chem. Soc.* **83**, 2799 (1961).
24. Ward, J. W., *J. Catal.* **9**, 225 (1967).
25. Le Francois, M., and Malbois, G., *J. Catal.* **20**, 350 (1971).
26. Hughes, T. R., and White, H. M., *J. Phys. Chem.* **71**(7), 2192 (1967).
27. Olah, G. A., "Freidel-Crafts Chemistry." Wiley, New York, 1973.